

# Imaging Upconverting Polymersomes in Cancer Cells: Biocompatible Antioxidants Brighten Triplet–Triplet Annihilation Upconversion

Sven H. C. Askes, Wim Pomp, Samantha L. Hopkins, Alexander Kros, Si Wu, Thomas Schmidt, and Sylvestre Bonnet\*

*Light upconversion is a very powerful tool in bioimaging as it can eliminate autofluorescence, increase imaging contrast, reduce irradiation damage, and increase excitation penetration depth in vivo. In particular, triplet–triplet annihilation upconverting (TTA-UC) nanoparticles and liposomes offer high upconversion efficiency at low excitation power. However, TTA-UC is quenched in air by oxygen, which also leads to the formation of toxic singlet oxygen. In this work, polyisobutylene-monomethyl polyethylene glycol block copolymers are synthesized and used for preparing polymersomes that upconvert red light into blue light in absence of oxygen. In addition, it is demonstrated that biocompatible antioxidants such as L-ascorbate, glutathionate, L-histidine, sulfite, trolox, or even opti-MEM medium, can be used to protect the TTA-UC process in these polymersomes resulting in red-to-blue upconversion under aerobic conditions. Most importantly, this approach is also functional in living cells. When A549 lung carcinoma cells are treated with TTA-UC polymersomes in the presence of  $5 \times 10^{-3}$  M ascorbate and glutathionate, upconversion in the living cells is one order of magnitude brighter than that observed without antioxidants. These results propose a simple chemical solution to the issue of oxygen sensitivity of TTA-UC, which is of paramount importance for the technological advancement of this technique in biology.*

S. H. C. Askes, Dr. S. L. Hopkins, Prof. A. Kros,  
Dr. S. Bonnet  
Leiden Institute of Chemistry  
Leiden University  
PO box 9502, 2300 RA Leiden, The Netherlands  
E-mail: bonnet@chem.leidenuniv.nl

W. Pomp, Prof. T. Schmidt  
Leiden Institute of Physics  
Leiden University  
PO box 9504, 2300 RA Leiden, The Netherlands  
Dr. S. Wu  
Max Planck Institute for Polymer Research  
55128 Mainz, Germany

This is an open access article under the terms of the Creative Commons Attribution-NonCommercial License, which permits use, distribution and reproduction in any medium, provided the original work is properly cited and is not used for commercial purposes.

DOI: 10.1002/sml.201601708



## 1. Introduction

Upconversion of light is the generation of high-energy photons from low-energy photons, for example, the conversion of red light to blue light. In biological systems, upconversion imaging is characterized by negligible autofluorescence, increased imaging contrast, reduced irradiation damage, and increased excitation penetration depth in vivo. Because of these advantages, lanthanoid-based upconverting nanoparticles (UCNPs), for example, have attracted extensive interest. However, UCNPs suffer from several disadvantages, such as the need for high excitation intensities or the low upconversion efficiencies observed in aqueous solution (typically  $\leq 0.5\%$ ), which results from the low absorption cross-section of lanthanoid ions and surface quenching by water.<sup>[1]</sup> In contrast, triplet–triplet annihilation upconversion (TTA-UC)

requires low excitation intensity (down to  $1 \text{ mW cm}^{-2}$ ), employs sensitizers having high molar absorptivity in the phototherapeutic window, resulting in upconversion quantum yields up to 14% in aqueous solution.<sup>[1,2]</sup> TTA-UC is based on the photophysical interplay of photosensitizer and annihilator chromophores (Figure S1, Supporting Information).<sup>[3]</sup> The photosensitizer absorbs low energy light, after which it intersystem crosses to a long-lived triplet state. This triplet state is transferred to the annihilator upon diffusional collision by means of triplet-triplet energy transfer (TTET); a succession of TTET leads to a buildup of long-lived triplet state annihilator molecules. Two triplet state annihilator molecules interact resulting in triplet-triplet annihilation upconversion, in which one of them departs with all the energy of the pair, thus reaching a high-energy singlet excited state. Finally, this singlet excited state returns to the ground state by fluorescent emission of a high-energy photon, thereby realizing upconversion. TTA-UC has been demonstrated in an extensive assortment of organic, inorganic, and/or supramolecular materials,<sup>[2b,4]</sup> as well as in nano- or micro-sized particles.<sup>[5]</sup> It has been used for applications in photocatalysis,<sup>[6]</sup> solar energy harvesting,<sup>[7]</sup> drug delivery and drug activation,<sup>[8]</sup> or bioimaging. In particular bioimaging using TTA-UC has been demonstrated, often in fixed cells, using silica-coated micelles,<sup>[1,9]</sup> dye-modified cellulose templates,<sup>[10]</sup> PMMA poly(methyl methacrylate) nanocapsules,<sup>[11]</sup> or soybean oil or oleic acid core nanocapsules.<sup>[12]</sup>

Although many published studies focusing on biological application of TTA-UC avoid discussing the sensitivity of their system to oxygen, TTA-UC inherently suffers from physical quenching of the sensitizer and/or annihilator triplet excited states by  $\text{O}_2$ . Such quenching leads to undesirable cytotoxic singlet oxygen, and concomitant loss of upconversion in the nanodevices. For example, the TTA-UC liposome system initially described by our group for the activation of a blue-light sensitive prodrug<sup>[8]</sup> functioned only under inert atmosphere. Other groups showed that TTA-UC bioimaging of PMMA nanocapsules in HeLa cells also suffered from oxygen sensitivity; in this case, upconversion was enhanced upon addition of valinomycin, which stimulates mitochondrial oxygen consumption.<sup>[11a]</sup> Here, we argue that addressing the issue of oxygen sensitivity is of paramount importance for the technological advancement of TTA-UC in biology. Using TTA-UC polymersomes, we demonstrate that it is possible to dramatically reduce the oxygen sensitivity of TTA-UC nano-sized systems by the addition of antioxidants, thereby creating a locally oxygen-depleted environment. Interestingly, this strategy can be applied to cell cultures as exemplified by the imaging of TTA-UC polymersomes inside living cancer cells.

The polymersomes used in this study belong to a large family of vesicles that have attracted significant attention in the fields of drug delivery and bioimaging research.<sup>[13]</sup> Polymersomes are typically composed of synthetic amphiphilic block copolymers that, similar to liposomes, self-assemble into spherical bilayer membranes surrounding an aqueous interior. Analogous to liposomes, the hydrophobic membrane of polymersomes can be doped with hydrophobic dyes such as palladium(II) tetraphenyl tetrabenzoporphyrin

(**1**) and 2,5,8,11-tetra(*tert*-butyl)perylene (**2**, see Figure 1). When combined, these dyes form a TTA-UC couple that is capable of upconverting red light into blue light. Polymersomes have many advantages compared to lipid-based liposomes. Notably, the membrane thickness, rigidity, fluidity, plasticity, permeability, and surface functionalization, can be tuned by choosing the appropriate copolymer. In addition, polymersomes typically feature high retention of encapsulates, high stability in aqueous media, and can be very cheap to make.<sup>[13a-d]</sup> In this study polyisobutylene (PiB,  $M_w \approx 1.0 \text{ kg mol}^{-1}$ ) and polyethylene glycol (PEG,  $M_w \approx 0.35$  or  $0.75 \text{ kg mol}^{-1}$ ) were chosen as the hydrophobic and hydrophilic polymer blocks, respectively.<sup>[14]</sup> PiB is a well-known polymer with low permeability to small molecules such as dioxygen; it has a high chemical and thermal resistance and a high biocompatibility.<sup>[15]</sup> PEG is a biocompatible polymer that has become an established standard for the surface functionalization of drug delivery and bioimaging systems. In this article, we describe the synthesis and characterization of upconverting PiB-PEG polymersomes, study the stability of red-to-blue TTA-UC in aqueous solution in presence of a range of biocompatible antioxidants, and demonstrate the enhanced TTA-UC imaging of these vesicles in living human cancer cells in presence of biocompatible antioxidants.

## 2. Results and Discussion

### 2.1. Synthesis and Characterization of TTA-Upconverting Polymersomes

In order to acquire a vesicle morphology, an amphiphilic block copolymer needs to have a hydrophilic block volume fraction of 0.25–0.45.<sup>[13b]</sup> Hence, two amphiphilic block copolymers (compounds **3** and **4**) were synthesized by condensation of polyisobutylene succinic anhydride (PiB-SA,  $M_w \approx 1.0 \text{ kg mol}^{-1}$ ) and monomethoxy polyethylene glycol ( $M_w \approx 0.35 \text{ kg mol}^{-1}$  for **3** and  $0.75 \text{ kg mol}^{-1}$  for **4**).<sup>[16]</sup> The products were characterized using NMR spectroscopy, IR spectroscopy, and gel-permeation chromatography (see the Experimental Section and the Supporting Information). Nanoparticle dispersions called **P3** and **P4** were produced with polymers **3** and **4**, respectively, using a freeze-thaw-extrusion protocol in phosphate buffered saline at a concentration of  $10 \text{ mg mL}^{-1}$  polymer. **P3** and **P4** were clear solutions that exhibited a typical nanoparticle scatter (Figure S11, Supporting Information). Sample **P3** was more opaque than **P4**, indicating a larger particle size. The hydrodynamic diameter (*z*-average) and polydispersity index (PDI) of the particles was measured using dynamic light scattering (DLS), with typical particle diameters of  $\approx 150$  and  $80 \text{ nm}$  for **P3** and **P4**, respectively, and PDI's ranging from 0.1 to 0.3 (Table 1). The nanoparticle dispersions were stable over time and the hydrodynamic radius did not change over a period of at least two months. The  $\zeta$ -potentials were  $-42.0$  and  $-24.0 \text{ mV}$  for **P3** and **P4**, respectively. The negative surface charge originates from the carboxylic acid groups in the polymer junction, which are deprotonated at neutral pH. The less negative

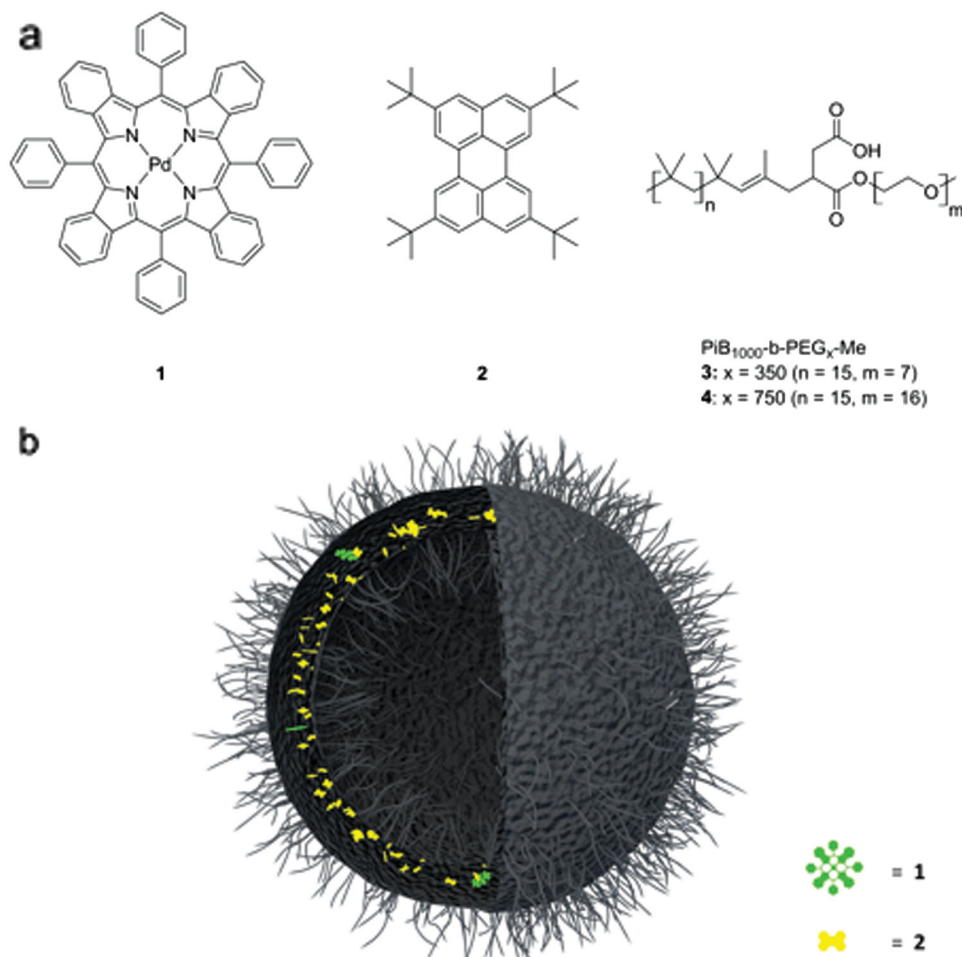


**Figure 1.** a) Chemical structures of the red photosensitizer palladium(II) tetraphenyl tetrabenzoporphyrin (**1**), of the blue emitter 2,5,8,11-tetra(*tert*-butyl)perylene (**2**), and of the polyisobutylene-block-monomethyl polyethylene glycol (PiB<sub>1000</sub>-b-PEG<sub>x</sub>-Me,  $x = 350$  or  $750$ ) amphiphilic block copolymers used in this study, with PiB molecular weight of  $1.0 \text{ kg mol}^{-1}$  and PEG block molecular weights of  $0.35 \text{ kg mol}^{-1}$  (**3**) and  $0.75 \text{ kg mol}^{-1}$  (**4**). b) Schematic illustration of a polymersome composed of **3** or **4**, and doped with compounds **1** and **2**.

charge of **P4** can be explained by the larger PEG-brush on its surface, which is known to decrease the observed surface charge due to an increased hydrodynamic drag.<sup>[17]</sup>

To examine the particle morphology and measure the particle diameter distribution, the samples were examined with transmission electron microscopy (TEM, see **Figure 2**).

The micrographs show that **P3** and **P4** consisted of particles of  $156 \pm 90 \text{ nm}$  (bimodal distribution) and  $95 \pm 49 \text{ nm}$  (unimodal distribution), respectively. Both populations were in close agreement with the DLS values. For both **P3** and **P4**, upon high-intensity exposure to the electron beam of the TEM microscope, the particle shell collapsed, liquid visibly

**Table 1.** Sample composition of all studied polymersome samples, and their typical particle sizes and surface charges; hydrodynamic particle diameters (z-average), polydispersity index (PDI),  $\zeta$ -potential, and particle diameters from transmission electron microscopy (TEM).  $\zeta$ -potentials were measured in 1:9 PBS:H<sub>2</sub>O at pH 7.1. All measurements were done at  $20^\circ\text{C}$ .

Sample	[3] [mg mL <sup>-1</sup> ]	[4] [mg mL <sup>-1</sup> ]	[1] [ $\times 10^{-6} \text{ M}$ ]	[2] [ $\times 10^{-6} \text{ M}$ ]	z-average [nm]	PDI	$\zeta$ -potential [mV]	TEM size [nm]
<b>P3</b>	10	–	–	–	149	0.120	$-42.0 \pm 7.5$	$156 \pm 90$
<b>P3-1</b>	10	–	10	–	152	0.136		
<b>P3-2</b>	10	–	–	200	154	0.154		
<b>P3-1-2</b>	10	–	10	200	146	0.189		
<b>P4</b>	–	10	–	–	83	0.263	$-24.0 \pm 10.7$	$95 \pm 49$
<b>P4-1</b>	–	10	10	–	83	0.277		
<b>P4-2</b>	–	10	–	200	86	0.267		
<b>P4-1-2</b>	–	10	10	200	77	0.263		

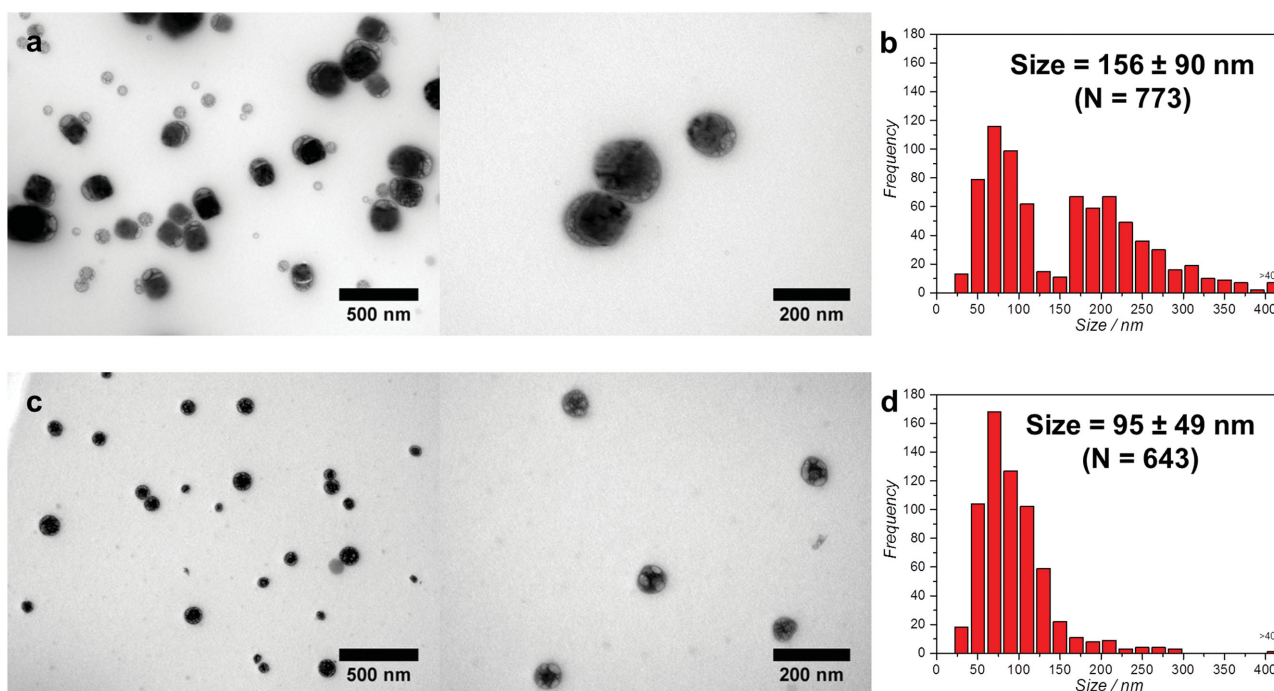


**Figure 2.** Transmission electron micrographs of a) **P3** and c) **P4** vesicles and b,d) their respective measured particle diameter distributions. The mean diameters and standard deviations were determined from a population ( $N$ ) of 773 and 643 individual particles for **P3** and **P4**, respectively.

leaked from the interior, and the particles became more and more translucent for electrons. After this transformation was complete, only an empty collapsed shell remained (Figure S8, Supporting Information). Surprisingly, the particles did not burst at low electron beam exposures, indicating that the shell successfully tolerated the high vacuum in the TEM chamber. Overall, these observations are consistent with vesicular nanoparticles composed of rubbery membranes surrounding an aqueous interior, i.e., polymersomes.

The TTA-UC dyes that were selected for incorporation in the polymersome membrane were palladium(II) tetraphenyl tetrabenzoporphyrin (**1**) as the red light-absorbing photosensitizer, and 2,5,8,11-tetra(*tert*-butyl)perylene (**2**) as the blue light-emitting annihilator. Instead of using the benchmark annihilator in many TTA-UC systems perylene,<sup>[3a]</sup> fourfold *tert*-butylated perylene was used to prevent aromatic stacking and thereby enhance solubility of the molecule in the hydrophobic environment of the membrane.<sup>[18]</sup> Preliminary experiments also indicated that the greater lipophilicity of **2** prevented the molecule from partitioning with the water phase in amphiphilic dispersions, whereas unsubstituted perylene shuttles between different membranes (data not shown).<sup>[19]</sup> With respect to perylene, the fluorescence maximum of **2** is reported to be bathochromically shifted by only about 15 nm while the fluorescence lifetime and quantum yield are very similar.<sup>[18,20]</sup> Indeed, this tetrasubstitution of perylene did not significantly alter the ability of this blue emitter to serve as an annihilator for red-to-blue TTA-UC. Bright red-to-blue TTA-UC was obtained in air by dissolving **1** and **2** in a 3:1 mixture of chloroform and oleic acid and illuminating with 50 mW 630 nm excitation ( $0.4 \text{ W cm}^{-2}$ ), without deoxygenation (Figure S9, Supporting Information). Next, **1** and/or **2** were incorporated

in polymersomes **P3** and **P4** resulting in dye-loaded polymersomes **P3-1**, **P3-2**, **P3-1-2**, **P4-1**, **P4-2**, and **P4-1-2** (see Table 1 for the membrane composition, and Figure 3 and Figure S11 (Supporting Information) for photographs of the samples). Both dyes were incorporated quantitatively in the vesicle membrane, and dye doping had no effect on particle size or stability (Table 1 and Figure 2). UV-vis absorption and emission spectroscopy with **P3-1**, **P3-2**, **P4-1**, and **P4-2** confirmed that both dyes were incorporated, with the dye absorbance and emission spectra being identical as compared to the isotropic chloroform solutions (compare Figure S10 with Figure S11 (Supporting Information)).

To demonstrate TTA-UC, polymersomes **P3-1-2** and **P4-1-2** were first investigated using UV-vis absorption and emission spectroscopy under aerobic conditions in the presence of 50 to  $75 \times 10^{-3} \text{ M}$  sodium sulfite (Figure 3). Sulfites are known scavengers of ground-state molecular oxygen.<sup>[8a,21]</sup> The UV-vis absorption spectrum shows the characteristic absorption bands of **1** (around 630 nm) and **2** (350–450 nm). At 20 °C and under red light excitation (at 630 nm, 50 mW,  $0.4 \text{ W cm}^{-2}$ ), the emission spectrum of both samples showed the typical phosphorescence band of **1** at 800 nm and the structured emission band of **2** at 460 nm (Figure 3c). These results represent the first example of TTA-UC in polymersomes. The upconversion emission was intense and could easily be viewed by the naked eye when the red excitation source was blocked with a 575 nm short-pass filter (Figure 3b). To study the location of TTA-UC, giant polymersomes **GP3-1-2** with a diameter of 5–10  $\mu\text{m}$  were assembled using the same constituents as in **P3-1-2**. Imaging using an optical microscope setup with 635 nm excitation and visualized from 450 to 575 nm confirmed that TTA-UC was indeed located in the polymer membrane (Figure S13, Supporting

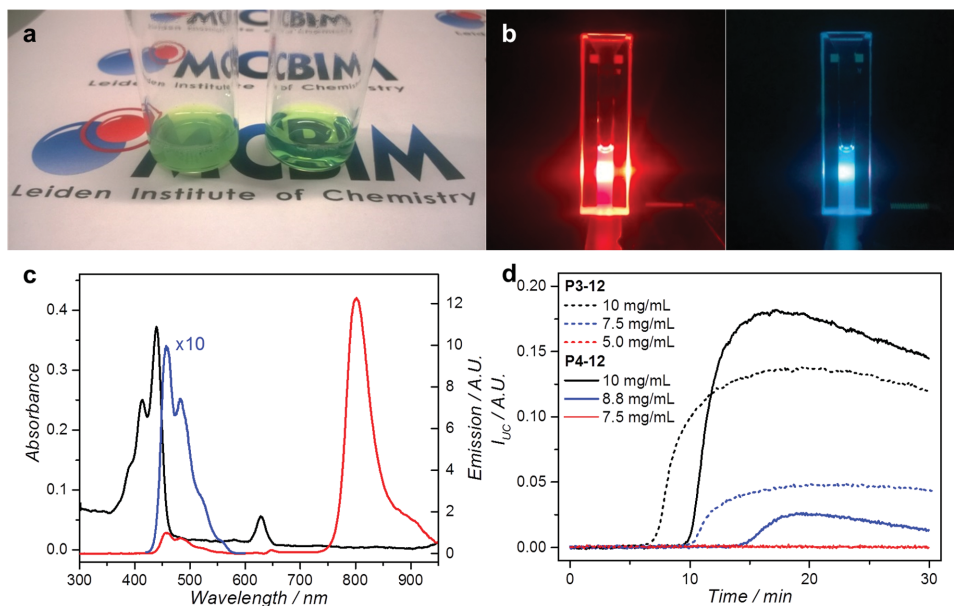


**Figure 3.** Visual and photophysical characterization of TTA-UC in **P3-1-2** and **P4-1-2**. a) Photographs of 10 mg mL<sup>-1</sup> dispersions of **P3-1-2** (left) and **P4-1-2** (right). b) Photographs of a 7.5 mg mL<sup>-1</sup> **P3-1-2** dispersion irradiated with a 50 mW 4 mm diameter red laser beam from the left side in presence of 75 × 10<sup>-3</sup> M sodium sulfite. In the right picture, the excitation source is blocked with a 575 nm short pass filter. c) UV-vis absorbance (black) and emission (red/blue) spectroscopy of **P4-1-2** vesicles (0.5 mg mL<sup>-1</sup> compound **4**) at 20 °C. Emission spectrum taken under red light irradiation (630 nm, 50 mW, 0.4 W cm<sup>-2</sup>) in presence of 50 × 10<sup>-3</sup> M sodium sulfite. For clarity, the blue curve is the red curve multiplied by 10. d)  $I_{UC}$  at 486 nm under red light irradiation (630 nm, 50 mW, 0.4 W cm<sup>-2</sup>, 4 mm excitation path length) of samples **P3-1-2** and **P4-1-2**. [3] = 10, 7.5, and 5.0 mg mL<sup>-1</sup> (dashed black, blue, and red, respectively), and [4] = 10, 8.8, and 7.5 mg mL<sup>-1</sup> (solid black, blue, and red, respectively). Conditions: 600 μL sample in a nonstirred semi-microcuvette at 20 °C. No oxygen scavenger was added here.

Information). The absolute quantum yield of upconversion ( $\Phi_{UC}$ ) in the polymersomes, measured using an integrating sphere setup (see the Experimental Section), amounted to 0.002 at 20 °C for both **P3-1-2** and **P4-1-2** (see Table 2). To investigate TTA-UC at human body temperature (37 °C), upconversion and phosphorescence were measured as a function of temperature between 5 and 50 °C (Figure S14, Supporting Information). Upon elevating the temperature, the upconversion emission gradually intensified ( $\Phi_{UC}$  at 37 °C = 0.005) while the phosphorescence intensity decreased. This evolution is beneficial for bioimaging at 37 °C. We attribute the higher TTA-UC efficiency at higher temperature to the higher mobility of **1** and **2** in the PiB membrane, as the translational diffusion rate of polyaromatic hydrocarbons in polyisobutylene materials is usually positively correlated to temperature.<sup>[22]</sup> The upconversion efficiency of **P3-1-2** and **P4-1-2** are in the same order of magnitude compared to red-to-blue TTA-UC in phospholipid-based liposomes

measured in similar conditions ( $\Phi_{UC}$  at 37 °C = 0.015% using perylene as annihilator).<sup>[8a]</sup> Finally, the intensity threshold ( $I_{th}$ ) at which the power dependency of upconversion changes from quadratic to linear was determined, as it is regarded as a benchmark parameter for the efficiency of TTA-UC.<sup>[2b,23]</sup> The red laser excitation power was varied between 16 and 510 mW cm<sup>-2</sup> while measuring the upconversion intensity at both 20 and 37 °C (Figure S15, Supporting Information). From the double logarithmic plot of upconversion intensity ( $I_{UC}$ ) versus excitation intensity ( $P$ ), a value of ca. 200 mW cm<sup>-2</sup> was determined for  $I_{th}$  at 20 °C (Table 2). At 37 °C,  $I_{th}$  decreased down to 20–50 mW cm<sup>-2</sup>, owing to the greater TTA-UC efficiency at this temperature. Note that excitation intensities above 200 mW cm<sup>-2</sup> can easily be reached in common laser microscopy setups. In summary, TTA-UC in polymersomes was established for the first time, and the photophysical characteristics were found compatible with biological imaging applications.

**Table 2.** Photophysical characteristics of **P3-1-2** and **P4-1-2** in presence of 50 × 10<sup>-3</sup> M sodium sulfite: absolute quantum yield of upconversion ( $\Phi_{UC}$ ) at 20 °C, ratio of upconversion emission intensity at 37 and 20 °C, estimation of  $\Phi_{UC}$  at 37 °C calculated from multiplying the intensity ratio  $I_{UC,37 °C}/I_{UC,20 °C}$  with  $\Phi_{UC}$  at 20 °C, and the intensity threshold ( $I_{th}$ ) for efficient TTA-UC at 20 and 37 °C.

Sample	$\Phi_{UC}$ at 20 °C [%]	$I_{UC,37 °C}/I_{UC,20 °C}$	Est. $\Phi_{UC}$ at 37 °C [%]	$I_{th}$ at 20 °C [mW cm <sup>-2</sup> ]	$I_{th}$ at 37 °C [mW cm <sup>-2</sup> ]
<b>P3-1-2</b>	0.20	2.7	0.54	256	204
<b>P4-1-2</b>	0.21	2.4	0.50	220	197

## 2.2. Do These Polymersome Dispersions Produce Upconversion in Air?

In liposomes based on saturated lipids such as DMPC (1,2-dimyristoyl-sn-glycero-3-phosphocholine), TTA-UC is inhibited by molecular oxygen, which physically quenches triplet excited states and results in the photocatalytic production of singlet oxygen. To investigate whether **P3-1-2** and **P4-1-2** were capable of producing upconversion under aerobic conditions, polymersome samples were prepared

without the oxygen scavenger sulfite at different copolymer bulk concentrations, and irradiated for 30 min while monitoring  $I_{UC}$  (Figure 3d, see Figures S16 and S18 in the Supporting Information for full datasets). For  $[3] = 10 \text{ mg mL}^{-1}$ , no upconversion was observed at  $t = 0$ , but after 7 min of red light irradiation, the band of upconverted blue light appeared and  $I_{UC}$  reached a maximum after  $\approx 15$  min irradiation. Comparison of the UV-vis absorbance spectra before and after irradiation showed significant bleaching of both dyes **1** and **2** (Figure S16, Supporting Information). No difference in DLS values were found before and after the experiment, indicating that red light irradiation did not damage the polymersomes' integrity. For  $[3] = 7.5 \text{ mg mL}^{-1}$ , the qualitatively identical observations were made but  $I_{UC}$  maximized at a lower value, whereas for  $[3] = 5 \text{ mg mL}^{-1}$ , no upconversion was observed at all after 30 min irradiation. As a control, a  $7.5 \text{ mg mL}^{-1}$  **P3-1-2** sample prepared in presence of  $75 \times 10^{-3} \text{ M}$  sodium sulfite exhibited a 1000-fold more intense upconversion band that was very stable over 30 min (Figure S17, Supporting Information). The results with **P4-1-2** vesicles were very similar: upconversion did not occur at polymer concentrations lower than  $8.8 \text{ mg mL}^{-1}$ . These results clearly indicated that in air TTA-UC in polymersomes was concentration-dependent. We interpret this result by the fact that the block-copolymers contain a C=C double bond that is known to be able to chemically quench singlet oxygen via a perepoxide mechanism.<sup>[24]</sup> We hypothesize that such chemical quenching results in the local consumption of oxygen during initial red light irradiation, up to the point where the oxygen concentration is low enough to allow TTA-UC to occur. At lower polymer concentrations, oxygen diffusion outcompetes its photochemical consumption, so that no upconversion was observed. Similar observations have been reported by Kim et al., who have used polyisobutylene as the liquid core in TTA-UC nanocapsules.<sup>[5a,25]</sup> To confirm this hypothesis, we repeated the experiment in a stirred macrocuvette with an oxygen sensor probing the oxygen concentration in solution (Figure S19, Supporting Information;  $[3] = [4] = 10 \text{ mg mL}^{-1}$ ). During red light irradiation, a gradual decrease in dissolved oxygen was indeed observed while upconversion first appeared after 15 min for **P3-1-2** and after 60 min for **P4-1-2**, i.e., when the bulk oxygen concentration was below 1–2 ppm. Overall, these results show that upconversion in polymersomes can indeed occur under air and in absence of sulfite, most likely due to singlet oxygen scavenging by the unsaturated polymer itself. However, under diluted conditions and thus reduced singlet oxygen scavenging capacity, upconversion in air does not occur anymore unless sulfite is added.

### 2.3. Addition of Other Water-Soluble Oxygen Scavengers to **P4-1-2**

Encouraged by these results, and realizing that TTA-UC in air can occur by chemical scavenging of ground state oxygen (sulfite) or singlet oxygen (copolymer alkene function), **P4-1-2** vesicles were mixed with a selection of known

antioxidants and irradiated with red light while continuously measuring oxygen concentration, the phosphorescence intensity  $I_{\text{phosphorescence}}$  (at 800 nm), and the upconversion intensity  $I_{UC}$  (at 486 nm, see Figure 4). The bulk copolymer concentration was fixed at  $0.5 \text{ mg mL}^{-1}$ , so that there would be no TTA-UC in air without antioxidants (see previous section). The antioxidants chosen were sodium sulfite, sodium ascorbate, sodium glutathionate, L-histidine, hydroquinone, and trolox, i.e., the water-soluble derivative of vitamin E. The antioxidant concentration was kept constant ( $10 \times 10^{-3} \text{ M}$  at pH 7.0–7.6) to mimic cellular concentrations of glutathione ( $0.5\text{--}10 \times 10^{-3} \text{ M}$ )<sup>[26]</sup> and thus there was an excess of it with respect to the dissolved oxygen concentration in an air-saturated aqueous solution at room temperature ( $\approx 9$  ppm;  $2.5 \times 10^{-3} \text{ M}$ ). In each of these experiments, as soon as the laser was switched on, a clear consumption of oxygen was observed, which decreased from  $\approx 8$  to 0 ppm in 15–25 min. In all cases, except for L-histidine, oxygen was already consumed in the dark, but illumination clearly accelerated the process, probably due to the higher redox potential of the  $^1\text{O}_2/\text{O}_2^{\bullet-}$  couple ( $E^0 = +0.65 \text{ V vs. NHE}$  at pH 7) compared to the  $^3\text{O}_2/\text{O}_2^{\bullet-}$  couple ( $E^0 = -0.33 \text{ V vs. NHE}$  at pH 7).<sup>[27]</sup> More importantly, the time evolution of emission showed a steep rise both for  $I_{UC}$  and  $I_{\text{phosphorescence}}$ , signifying the stabilization of the triplet excited states at sufficiently low oxygen concentrations. Strong TTA-UC was observed instantaneously (within 30 s) for sodium sulfite, sodium ascorbate, L-histidine, and trolox. For sodium glutathionate, upconversion was first observed after 2 min. Upconversion could not be observed in mixtures with hydroquinone, even at 0 ppm oxygen concentrations. We explain this result by the fact that the reaction of hydroquinone and oxygen produces benzoquinone, which is known to quench the triplet excited states of aromatic hydrocarbons due to charge-transfer interactions.<sup>[28]</sup> As control experiments, irradiation at identical conditions was repeated without oxygen scavengers, and without oxygen scavengers in the dark (Figure S20, Supporting Information). As expected, no oxygen consumption or upconversion was observed. Additionally, a physical quencher of singlet oxygen, i.e., sodium azide,<sup>[29]</sup> was tested as well. In presence of  $10 \times 10^{-3} \text{ M NaN}_3$  however (Figure 4), no UC and only weak phosphorescence were observed, which confirmed that chemical quenching is required for obtaining TTA-UC, rather than physical quenching. Finally, upconversion in **P4-1-2** vesicles was also tested in a 1:19 v/v mixture of vesicles and opti-MEM cell medium, which also contains biocompatible antioxidants (see formulation in the Experimental Section). Upconversion was first detected after 6 min irradiation and dissolved oxygen was depleted within 20 min irradiation, which confirmed the presence of chemical quenchers of singlet oxygen in the medium (probably sodium pyruvate and bovine serum albumin from fetal calf serum).<sup>[30]</sup> Overall, these results clearly demonstrate that the addition of a biologically realistic concentration of antioxidants is a potent strategy to obtain TTA-UC in air. The local  $\text{O}_2$  concentration is depleted by chemically consuming either ground-state oxygen (sulfite) or the photocatalytically generated singlet oxygen (histidine, etc.), until an oxygen threshold is reached where TTA-UC becomes possible.

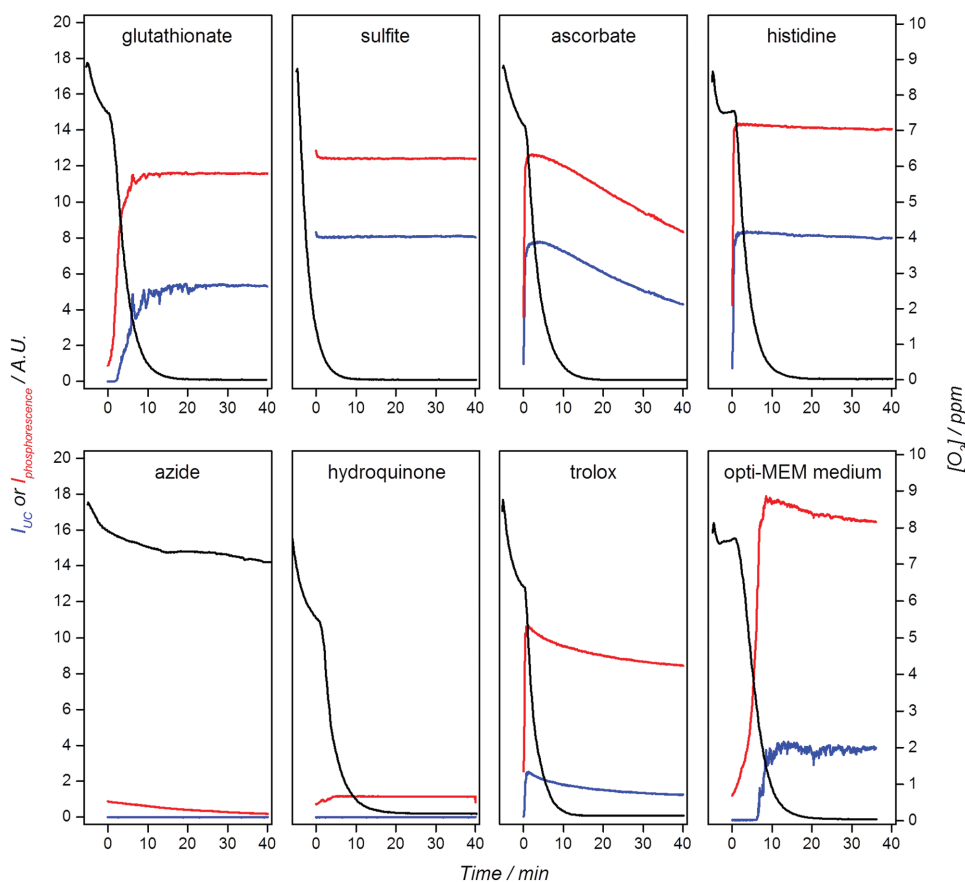


**Figure 4.** Emission (red/blue) and oxygen concentration (black) time traces of polymersome **P4-1-2** samples in air under red light irradiation ( $630\text{ nm}$ ,  $50\text{ mW}$ ,  $0.4\text{ W cm}^{-2}$ ) irradiation with addition of  $10 \times 10^{-3}\text{ M}$  sodium glutathionate, sodium sulfite, sodium ascorbate, L-histidine, sodium azide, hydroquinone, trolox, or 1:19 v/v mixed with opti-MEM cell culture medium (see formulation in the Experimental Section). Red and blue lines represent  $I_{\text{phosphorescence}}$  (at  $800\text{ nm}$ ) and  $I_{\text{UC}}$  (at  $486\text{ nm}$ , multiplied by 10 for clarity), respectively. Conditions:  $[4] = 0.5\text{ mg mL}^{-1}$ ,  $[1] = 0.5 \times 10^{-6}\text{ M}$ ,  $[2] = 10 \times 10^{-6}\text{ M}$ ,  $T = 20\text{ }^{\circ}\text{C}$ ,  $\text{pH} = 7.0\text{--}7.3$  ( $\text{pH}$  for the trolox experiment was 7.6 to dissolve the compound completely), with a  $2\text{ mL}$  sample volume in a stirred macrocuvette. Laser was turned on at  $t = 0$ .

## 2.4. Antioxidants Brighten TTA-UC in Cancer Cell Cultures

To see whether these results are also valid in cell culture conditions using live cells, human lung carcinoma A549 cells were incubated with **P4-1-2** for 4 h, in the absence or presence of a mixture of  $5 \times 10^{-3}\text{ M}$  sodium ascorbate and sodium glutathionate as antioxidant “cocktail.” After refreshing the medium and staining the nuclei with Hoechst 33342, the cells were visualized with optical microscopy at  $37\text{ }^{\circ}\text{C}$ ,  $7\%\text{ CO}_2$ , and  $1\%\text{ O}_2$  (**Figure 5**). An atmosphere with a low oxygen concentration was chosen to mimic median tumor oxygen partial pressures, which generally range from  $0.5\%$  to  $4\%$  ( $\text{pO}_2 = 5\text{--}30\text{ mm Hg}$ ).<sup>[31]</sup> In absence of antioxidants and under  $405\text{ nm}$  excitation, fluorescent spots were detected in the cytosol that correspond to singlet emission of **2** in the polymersomes. Under the hypothesis that nanoparticles are usually endocytosed,<sup>[32]</sup> we tentatively assigned these spots to be endosomes, lysosomes, and/or multivesicular bodies containing the polymersomes. Attempts were undertaken to demonstrate the colocalization of these spots and endo- or lysosomes using LysoTracker Red, but the rapid motion of these fluorescent spots during imaging prevented a conclusive outcome. Under  $635\text{ nm}$  excitation, upconverted emission

was detected in locations that closely matched the emission detected under  $405\text{ nm}$  irradiation (Figure S21, Supporting Information). Considering that upconversion only occurs when **1** and **2** are colocated in the same membrane, this observation indicates that the polymersomes were still intact and located where upconversion was detected. However, the upconversion emission intensity was rather weak and sometimes difficult to detect at all.

In contrast, when the cells were incubated with the antioxidants cocktail described above, very similar images for the bright field and  $405\text{ nm}$  excitation were obtained. However, a much brighter image was obtained upon  $635\text{ nm}$  excitation with  $1\%\text{ O}_2$ . Imaging was also performed at  $19\%\text{ O}_2$  and  $7\%\text{ CO}_2$  (i.e.,  $\text{pO}_2$  far exceeding any in vivo tissue oxygenation level), but no upconversion emission was detected at all under these conditions (data not shown). To quantify the emission at  $1\%\text{ O}_2$ , 30 individual image sets with  $40\times$  magnification were acquired in the presence and absence of antioxidants (10–20 cells per image, see the Experimental Section and Figure S22 (Supporting Information)), and the emission was quantified by calculating the mean pixel value of each image (Figure 5b,c). While the emission intensity with  $\lambda_{\text{exc}} = 405\text{ nm}$ , and thus the

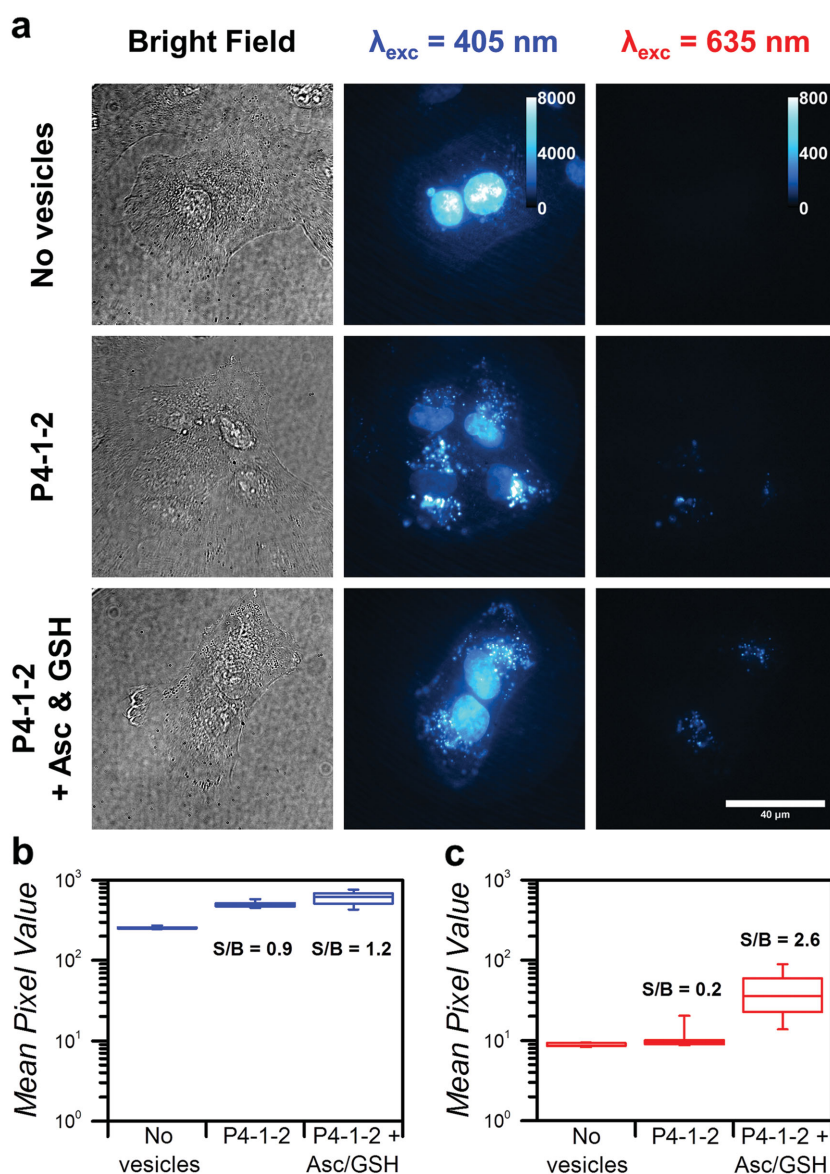


**Figure 5.** In vitro upconversion imaging using **P4-1-2** polymersomes. a) Imaging of **P4-1-2** upconverting polymersomes in living A549 lung carcinoma cells in bright field mode (left column), with  $\lambda_{\text{exc}} = 405 \text{ nm}$  (middle column), and with  $\lambda_{\text{exc}} = 635 \text{ nm}$  (right column) with 100 $\times$  magnification. Cells were incubated for 4 h with Opti-MEM only (top row), with 1:1 v/v mixture of Opti-MEM and **P4-1-2** vesicles ([**4**] = 0.5 mg mL<sup>-1</sup>), or with 1:1 v/v mixture of Opti-MEM and **P4-1-2** vesicles ([**4**] = 0.5 mg mL<sup>-1</sup>) and addition of 5  $\times$  10<sup>-3</sup> M sodium ascorbate and 5  $\times$  10<sup>-3</sup> M sodium glutathionate (bottom row). The cell nuclei were stained with Hoechst 33342 prior to imaging (1  $\mu\text{g mL}^{-1}$  in PBS, incubated for 20 min). Imaging conditions:  $T = 37 \text{ }^\circ\text{C}$ , 7.0% CO<sub>2</sub>, 1.0% O<sub>2</sub>, 62  $\mu\text{W}$  405 nm laser power (60  $\mu\text{m}$  spot diameter, 2.2 W cm<sup>-2</sup> intensity), 13 mW 635 nm laser power (50  $\mu\text{m}$  spot diameter, 640 W cm<sup>-2</sup> intensity), cells were allowed to equilibrate for 30 min before imaging. For comparison, the image histograms for  $\lambda_{\text{exc}} = 405 \text{ nm}$  are scaled from 0 to 8000 pixel values, and for  $\lambda_{\text{exc}} = 635 \text{ nm}$  are scaled from 0 to 800 pixel values, as indicated by the calibration bars in the top row. b,c) Quantified fluorescence emission under 405 nm (b) and 635 nm (c) excitation. The emission was quantified as the mean pixel value, based on 30 individual images at 40 $\times$  magnification for each experiment, without nuclear stain, see the Experimental Section and Figure S22 (Supporting Information). Mean signal to background ratios ( $S/B$ ) are given for both 405 and 635 nm excitation as the ratio of the mean luminescence intensity and the mean background intensity (i.e., the “No vesicles” dataset).

uptake of polymersomes, was not influenced by the addition of antioxidants, the upconversion emission ( $\lambda_{\text{exc}} = 635 \text{ nm}$ ) was found to be an order of magnitude more intense in

the applicability of TTA-UC bioimaging nanoparticles and may open new routes toward the application of TTA-UC for phototherapy.

presence of the antioxidant cocktail. The mean signal to background ratio ( $S/B$ , see the Experimental Section for definition) increased from 0.2 (without antioxidant) to 2.6 (with antioxidant, see Figure 5c). By contrast, the  $S/B$  ratio for  $\lambda_{\text{exc}} = 405 \text{ nm}$  remained low ( $\approx 1$ ) due to substantial autofluorescence of the cells, and it was not influenced by the presence of the antioxidant cocktail (Figure 5b). These exciting results demonstrate the potential of TTA-UC polymersomes for bioimaging. Indeed, in vitro data mirror the data obtained in homogeneous solution, which demonstrate that cotreatment with cell-compatible antioxidants, at oxygen concentration that are realistic for tumor environments, brighten TTA-UC in living human cancer cells.

### 3. Conclusion

TTA-UC polymersomes were constructed in aqueous buffers by self-assembly of polyisobutylene-*b*-monomethoxy polyethylene glycol block-copolymers (PiB-*b*-PEG-Me, **3** or **4**), a red-light absorbing porphyrin photosensitizer **1**, and a blue-light emitting tert-butylated perylene annihilator **2**. Only weak red-to-blue upconversion was observed in concentrated dispersions in air, and dilution completely abolished upconversion emission. However, upon the addition of chemical antioxidants such as sulfite, ascorbate, glutathionate, l-histidine, or trolox, intense and stable upconversion was observed in air (21% O<sub>2</sub>) for minutes or even hours. Scavenging of reactive oxygen species by the sacrificial antioxidant led to an oxygen-depleted environment in the illuminated area where TTA-UC can occur efficiently. The biocompatibility of this strategy was demonstrated by incubating these polymersomes in vitro in the absence or presence of a mixture of ascorbate and glutathionate. The upconversion luminescence was one order of magnitude more intense when the cells were cotreated with the antioxidants cocktail. These results clearly demonstrate that biocompatible antioxidants brighten TTA-UC not only in aqueous solution, but also in living cancer cells. These results reinforce

## 4. Experimental Section

**General:** Polyisobutylene succinic anhydride (PiB<sub>1000</sub>-SA, Dove-mulse H1000) with a saponification number of 58.1 mg KOH g<sup>-1</sup> was kindly provided by DoverChem (Dover, OH, USA) and was purified by silica flash chromatography in pure DCM (dichloromethane) before use. Palladium tetraphenyltetrabenzoporphyrin (**1**) was purchased from Bio-Connect (Huissen, The Netherlands). Dulbecco's phosphate buffered saline (DPBS) was purchased from Sigma-Aldrich and had a formulation of 8 g L<sup>-1</sup> NaCl, 0.2 g L<sup>-1</sup> KCl, 0.2 g L<sup>-1</sup> KH<sub>2</sub>PO<sub>4</sub>, and 1.15 g L<sup>-1</sup> K<sub>2</sub>HPO<sub>4</sub> with a pH of 7.1–7.5. All other chemicals were purchased from major chemical suppliers and used as received.

The average polymersome diameter, polydispersity index, and zeta-potential were measured using a Malvern Instruments Zetasizer Nano-S machine, operating with a wavelength of 632 nm. The zeta-potential measurement was carried out in a DTS1070 folded capillary cell. Transmission electron microscopy was done on a Jeol 1010 with an acceleration voltage of 80 kV. Images were collected with an Olympus Megaview G2 camera, and Olympus iTEM software. Samples were loaded on Formvar/Carbon film on Copper 400 mesh TEM grids (FC400Cu100; van Loenen Instruments, Zaandam, The Netherlands). Oxygen measurements were done with an Ocean Optics NeoFox Foxy oxygen probe that was calibrated with 1 M Na<sub>2</sub>SO<sub>3</sub> as the zero-oxygen point. Images and data were processed using Fiji ImageJ,<sup>[33]</sup> Origin Pro, and/or Micro-soft Excel software.

**Synthesis of 2,5,8,11-Tetra(tert-butyl)perylene (Compound 2):** Adapted from literature procedures.<sup>[34]</sup> 0.50 g perylene (1.98 mmol) was added to 50 mL dry tert-butyl chloride under Schlenk conditions. 1.0 g anhydrous aluminum trichloride was added and the mixture was refluxed for 6 h, after which an additional 30 mL tert-butyl chloride was added and the mixture was further refluxed overnight. Then, 20 mL tert-butyl chloride and 1.0 g anhydrous aluminum trichloride were added and reflux was continued for another 24 h. The mixture was allowed to cool to room temperature and extracted with 100 mL brine in a separatory funnel. The aqueous layer was separated and extracted with three 50 mL portions of DCM. The DCM fractions were combined with the previously obtained organic fraction and dried with anhydrous sodium sulfate. The dried organic layer was filtered and rotary-evaporated at 80 °C until a concentrate remained, which was baked in a petri-dish on a hot plate at 170 °C for 30 h, at which point smoke ceased to evolve. The remaining dark brown solid was dissolved in a 2:1 mixture of petroleum ether and chloroform and purified with silica column chromatography (gradient of pure PE to 2:1 PE:CHCl<sub>3</sub> mixture, R<sub>f</sub> = 0.93 in PE:CHCl<sub>3</sub>) to afford 0.72 g of orange crystalline product (1.51 mmol, 76%). An aliquot of the product was recrystallized from 50:50 DCM:MeOH for use in photophysical experiments. <sup>1</sup>H NMR (300 MHz, CDCl<sub>3</sub>) δ (ppm) 8.24 (d, J = 1.7 Hz, 4 H), 7.63 (d, J = 1.6 Hz, 4 H), 1.50 (s, 36 H). <sup>13</sup>C NMR (75 MHz, CDCl<sub>3</sub>) δ (ppm) 148.8, 135.0, 130.9, 125.9, 123.4, 117.8, 35.0, 31.5. NMR spectra matched literature data.<sup>[35]</sup>

**Synthesis of PiB<sub>1000</sub>-b-PEG<sub>350</sub>-Me (Compound 3):** Adapted from literature procedure, see Scheme S1 (Supporting Information).<sup>[16]</sup> 3.66 g PiB<sub>1000</sub>-SA (3.79 mmol) and 1.32 g monomethoxy PEG<sub>350</sub> (3.77 mmol) were heated to 80 °C, blanketed with argon by three cycles of evacuation and argon purging, and then stirred overnight at 110–120 °C. The mixture was allowed to cool to room

temperature, after which it was purified by silica column chromatography (DCM:MeOH gradient from 99:1 to 95:5; R<sub>f</sub> = 0.37 for 95:5 DCM:MeOH) to yield 2.89 g of product (2.08 mmol, 55%). <sup>1</sup>H NMR (400 MHz, CDCl<sub>3</sub>) δ (ppm) 4.9–4.8 (1 H, C=C of PiB), 4.3–4.1 (2 H, alpha protons of the ester), 3.8–3.5 (30 H, PEG) 3.4 (3 H, O–CH<sub>3</sub> of PEG-Me), 3.1–2.9; 2.8–2.4; 2.3–2.1; 2.1–0.8 (111 H, methyl and methylene of PiB). IR spectroscopy (cm<sup>-1</sup>): 3467 (OH), 2949, 2883 (C–H), 1734 (C=O), 1638 (C=C), 1470, 1389, 1366, 1231 (PiB skeleton), and 1104 (C–O of PEG). NMR and IR spectra were given in Figures S4 and S6 (Supporting Information), respectively, both corresponding to literature data.<sup>[16]</sup> Gel permeation chromatogram was given in Figure S2 (Supporting Information). MALDI-TOF (matrix assisted laser desorption ionization time-of-flight) mass spectrometry did not yield a usable spectrum.

**Synthesis of PiB<sub>1000</sub>-b-PEG<sub>750</sub>-Me (Compound 4):** Identical procedure followed as for PiB<sub>1000</sub>-PEG<sub>350</sub>-Me. Used 1.87 g PiB<sub>1000</sub>-SA (1.81 mmol) and 1.29 g monomethoxy PEG<sub>750</sub> (1.72 mmol). 1.79 g product obtained (1.00 mmol, 59%). R<sub>f</sub> = 0.29 for 95:5 DCM:MeOH. <sup>1</sup>H NMR (400 MHz, CDCl<sub>3</sub>) δ (ppm) 4.9–4.8 (1 H, C=C of PiB), 4.3–4.1 (2 H, alpha protons of the ester), 3.8–3.5 (71 H, PEG) 3.4 (3 H, O–CH<sub>3</sub> of PEG-Me), 3.1–2.9; 2.8–2.4; 2.3–2.1; 2.1–0.8 (169 H, methyl and methylene of PiB). IR spectroscopy (cm<sup>-1</sup>): 3487 (OH), 2949, 2878 (C–H), 1737 (C=O), 1636 (C=C), 1470, 1388, 1366, 1230 (PiB skeleton), and 1107 (C–O of PEG). NMR and IR spectra were given in Figures S5 and S7 (Supporting Information), respectively, both corresponding to literature data.<sup>[16]</sup> Gel permeation chromatogram was given in Figure S3 (Supporting Information). MALDI-TOF mass spectrometry did not yield a usable spectrum.

**Preparation of Upconverting Polymersomes:** Polymersomes and dye-doped polymersomes were prepared according to a hydration-extrusion protocol. As an example, the preparation of **P4-1-2** was described here. Aliquots of chloroform stock solutions containing the polymersome constituents were added together in a glass tube to obtain a solution with 10 mg PiB<sub>1000</sub>-PEG<sub>750</sub>-Me, 10 nmol palladium tetraphenyltetrabenzoporphyrin (**1**), and 200 nmol 2,5,8,11-tetra(tert-butyl)perylene (**2**). The organic solvent was removed by rotary evaporation and subsequently under high vacuum for at least 15 min to create a polymer film. 1.0 mL DPBS buffer was added and the polymer film was hydrated by three cycles of freezing the flask in liquid nitrogen and thawing in warm water (50 °C). The resulting dispersion was extruded through a Whatman Nuclepore 0.1 μm polycarbonate filter at room temperature at least 11 times using a mini-extruder from Avanti Polar Lipids, Inc. (Alabaster, Alabama, USA). The number of extrusions was always odd to prevent any unextruded material ending up in the final liposome sample. The extrusion filter remained completely colorless after extrusion, suggesting full inclusion of the chromophoric compounds in the polymer membrane. Polymersomes were stored at room temperature and were typically used for further experiments within 24 h. The polymersomes were characterized with DLS, zeta potentiometry, and transmission electron microscopy.

**Preparation of Giant Polymersomes:** All giant polymersomes were prepared by lipid film rehydration on dextran chemically cross-linked hydrogel substrates by a method described elsewhere.<sup>[21a,36]</sup> The preparation of **GP3-1-2** was described here as an example. Glass microscopy slides were first incubated with 1:1 vol MeOH:HCl (37%) for 30 min, then with 98% H<sub>2</sub>SO<sub>4</sub> for

30 min, and then thiol-functionalized by incubating them for 1 h in a 2 wt% solution of (3-mercaptopropyl)triethoxysilane in dry toluene under a nitrogen atmosphere, and washing them three times with toluene. Directly after, a homogeneous film of Dex-PEG hydrogel was formed on this surface by drop-casting 600  $\mu\text{L}$  of a 1:1 volume mixture of 2 wt% maleimide-functionalized dextran, with a substitution degree of three maleimide groups per 100 glucopyranose residues of dextran (synthesis and characterization were detailed in ref. [2]), in water and 2 wt%  $\alpha,\omega$ -PEG dithiol (1500  $\text{g mol}^{-1}$ ) in water at room temperature. A homogeneous hydrogel film was formed after 30–45 min at 40 °C. Then, 10  $\mu\text{L}$  of polymer mixture stock solution in chloroform, containing 10  $\text{mg mL}^{-1}$  **3**,  $0.20 \times 10^{-3}$  M **2**, and  $10 \times 10^{-6}$  M **1**, was deposited on the hydrogel surface. The organic solvent dried within 1 min, after which the slide was dried further for at least 20 min under vacuum at room temperature. The polymer film was then hydrated with 400  $\mu\text{L}$  0.2 M sucrose in phosphate buffered saline (PBS) for 1 h at 50 °C, creating a buffered solution containing free-floating vesicles. For optical microscopy imaging, 300  $\mu\text{L}$  of this solution was transferred to an Eppendorf tube containing 700  $\mu\text{L}$  0.2 M glucose in PBS to allow the sucrose-loaded giant vesicles to sink to the bottom of the tube. After 1 h, 300  $\mu\text{L}$  of this giant polymersome sediment was transferred to a visualization microscopy chamber, and the rest of the chamber was filled with 100  $\mu\text{L}$  0.2 M glucose PBS. Finally, to chemically deoxygenate the chamber, 100  $\mu\text{L}$  0.5 M sodium sulfite in PBS was added. The vesicles were imaged within 24 h with a modified epifluorescence microscope setup, see below.

**Emission Spectroscopy:** Emission spectroscopy was conducted in a custom-built setup (Figure S23, Supporting Information). All optical parts were connected with FC-UVxxx-2 ( $xxx = 200, 400, 600$ ) optical fibres from Avantes (Apeldoorn, The Netherlands), with a diameter of 200–600  $\mu\text{m}$ , respectively, and that were suitable for the UV–vis range (200–800 nm). Typically, 2.0 mL of sample was placed in a 111-OS macrofluorescence cuvette from Hellma in a CUV-UV/VIS-TC temperature-controlled cuvette holder with stirring from Avantes. The cuvette holder temperature was controlled with a TC-125 controller and T-app computer software from Quantum Northwest (Liberty Lake, WA, USA), while the sample temperature was measured with an Omega RDXL4SD thermometer with a K-type probe submerged in the sample. The sample was excited with a collimated 630 nm laser light beam (4 mm beam diameter) from a clinical grade Diomed 630 nm PDT laser. The 630 nm light was filtered through a FB630-10, 630 nm band pass filter (Thorlabs, Dachau/Munich, Germany) put between the laser and the sample. The excitation power was controlled using the laser control in combination with a NDL-25C-4 variable neutral density filter (Thorlabs), and measured using a S310C thermal sensor connected to a PM100USB power meter (Thorlabs). For regular measurements, the excitation power was set at a power of 50 mW ( $0.4 \text{ W cm}^{-2}$ ). UV–vis absorption spectra were measured using an Avalight-DHc halogen-deuterium lamp (Avantes) as light source and a 2048L StarLine spectrometer (Avantes) as detector, both connected to the cuvette holder at a 180° angle and both at a 90° angle with respect to the red laser irradiation direction. The filter holder between cuvette holder and detector was in a position without a filter (Figure S23, Supporting Information, item 8). Luminescence emission spectra were measured using the same detector but with the UV–vis light source switched off. To visualize the spectrum

from 550 to 900 nm, while blocking the red excitation light, a Thorlabs NF-633 notch filter was used in the variable filter holder. To visualize the spectrum from 400 to 550 nm, an OD4 575 nm short pass filter (Edmund Optics, York, UK, part no. 84-709) was used. All spectra were recorded with Avasoft software from Avantes and further processed with Microsoft Office Excel 2010 and Origin Pro software. The emission spectra obtained from the two filters were stitched together at 550 nm to obtain a continuous spectrum from 400 to 900 nm. No correction was needed to seamlessly connect the spectra.

**Determination of the Quantum Yield of Upconversion:** The quantum yield of upconversion was determined absolutely by means of an integrating sphere setup. The setup and measurement procedure are discussed in depth in the Supporting Information.

**General Cell Culturing:** A549 human lung carcinoma cells were cultured in 25  $\text{cm}^2$  flasks in 8 mL Dulbecco's Modified Eagle Medium with phenol red (Sigma Life Science, USA), supplemented with 8.2% v/v fetal calf serum (FCS; Hyclone), 200  $\text{mg L}^{-1}$  penicillin and streptomycin (P/S; Duchefa), and  $1.8 \times 10^{-3}$  M glutamine-S (GM; Gibco, USA), under standard culturing conditions (humidified, 37 °C atmosphere containing 7.0%  $\text{CO}_2$ ). The cells were split approximately once per week upon reaching 70%–80% confluency, using seeding densities of  $2 \times 10^5$  cells and the medium was refreshed once per week. Cells were passaged for four to eight weeks.

**Cell Imaging Preparation:** After cell splitting, the cells were suspended in OptiMEM (Life Technologies, USA), supplemented with 2.5% FCS, 200  $\text{mg L}^{-1}$  P/S, and  $1.8 \times 10^{-3}$  M GM at  $3 \times 10^5$  cells per mL. For imaging at 100 $\times$  magnification, 100  $\mu\text{L}$  of this suspension was placed in a droplet on round 25 mm diameter microscopy coverslips (VWR, thickness no. 1) in a 6-well plate. After 5 min of sedimentation, 3 mL OptiMEM was carefully added to each well, and the cells were incubated for 24 h. For imaging at 40 $\times$  magnification, cells were seeded in a glass-bottom 24-well plate (Greiner Bio-One International, Germany, item no. 662892) at 50k cells per well and incubated for 24 h. Meanwhile, **P4-1-2** polymersome samples were prepared as before (**[4]** = 10  $\text{mg mL}^{-1}$ , 1 mL volume), and then purified by size exclusion chromatography (NAP-25 columns from GE healthcare, PBS as eluents) by collecting only the green eluting band ( $\approx 2$  mL), and diluting this elute further to a volume of 10.0 mL with PBS. Optionally, this final PBS solution contained  $20 \times 10^{-3}$  M sodium ascorbate and  $20 \times 10^{-3}$  M sodium glutathionate. Then, the solution was sterilized with a 0.2  $\mu\text{m}$  filter and diluted with 10 mL Opti-MEM (**[4]** = 0.5  $\text{mg mL}^{-1}$ ). 3 mL of this solution was added to each well of the 6-well plate, and the cells were incubated for 4 h. Then, the cells were washed once with PBS, and resupplied with 1 mL Opti-MEM before imaging. Optionally, the cells were incubated with 1  $\mu\text{g mL}^{-1}$  Hoechst 33342 in PBS for 20 min at 37 °C to stain the cell nuclei.

**Cell and Giant Polymersome Imaging:** Bright field and (upconversion) emission imaging was performed with a customized Zeiss Axiovert S100 Inverted Microscope setup, fitted with a Zeiss 100 $\times$  Plan Apochromat 1.4 NA oil objective or a Zeiss 40 $\times$  EC Plan Neofluar 1.3 NA oil objective, and an Orca Flash 4.0 V2 sCMOS (scientific complementary metal oxide semiconductor) camera from Hamamatsu, which together produced 4.2 megapixel images with pixel size of 69 nm (for 100 $\times$ ) or 173 nm (for 40 $\times$ ). The typical camera exposure time was 1000 ms. Samples were loaded in a temperature and atmosphere controlled

stage-top mini-incubator (Tokai Hit, Japan) set at 37 °C with 1% O<sub>2</sub> and 7% CO<sub>2</sub> in which samples were incubated for 30 min before imaging. For imaging at 100× magnification, a custom-made sample holder for round 25 mm cover slips was used. For direct excitation and fluorescence imaging of **2**, a CrystaLaser DL-405-050 405 nm solid state laser was used, combined with a ZT405/514/561rpc dichroic beam splitter (Chroma Technology Corporation) and ZET442/514/568m emission filter (Chroma Technology Corporation). The output power of the 405 nm laser at the sample was typically 62 μW at 100× magnification (60 μm spot diameter, intensity 2.2 W cm<sup>-2</sup>) and 76 μW at 40× magnification (150 μm spot diameter, intensity 0.44 W cm<sup>-2</sup>). For upconversion emission microscopy, a LRD-0635-PFR-00200-01 LabSpec 635 nm Collimated Diode Laser (Laserglow Technologies, Toronto, Canada) was used as excitation source, combined with a Chroma ZT405/532/635rpc dichroic beam splitter. To block everything except upconversion emission, a 575 nm short pass filter (Edmund Optics, part no. #84-709) was placed between the sample and the camera, resulting in OD > 5 at 635 nm and 800 nm (i.e., the excitation source and the phosphorescence of **1** were completely blocked). The output power of the 635 nm laser at the sample was typically 12.6 mW at 100× magnification (50 μm spot diameter, intensity 640 W cm<sup>-2</sup>) and 13.1 mW at 40× magnification (131 μm spot diameter, intensity 97 W cm<sup>-2</sup>). All laser beam spots had a Gaussian intensity profile; spot diameters were reported as Full Width at Half Maximum values.

**Quantification of Luminescence:** The mean total signal ( $S_T$ ) of the images was defined as

$$S_T = BG + L \quad (1)$$

where  $BG$  was the mean background signal and  $L$  was the mean luminescence signal.  $BG$  was measured in absence of P4-12 (i.e.,  $L = 0$ ).  $S_T$  was calculated in mean pixel value by taking the sum of all pixel values ( $V$ ) in the region of interest (ROI), containing a certain amount of pixels (px), and dividing by the ROI area ( $A_{ROI}$ , in px)

$$S_T = \frac{\sum_{px \in ROI} V_{px}}{A_{ROI}} \quad (2)$$

The same ROI was used for all images with a 1200 px diameter, closely encircling the illumination spot, see Figure S22 (Supporting Information). The cell confluency in the illumination spot was always 70%–100%, amounting to 10–20 cells located in the ROI.  $S_T$  was calculated for 30 individual images of each experiment (300 to 600 individual cells) by measuring the mean pixel value within the ROI with Fiji ImageJ software.<sup>[33]</sup> The mean signal to background ratio ( $S/B$ ) was then calculated from the  $S_T$  and  $BG$  values

$$S/B = \frac{L}{BG} = \frac{S_T - BG}{BG} \quad (3)$$

## Supporting Information

Supporting Information is available from the Wiley Online Library or from the author.

## Acknowledgements

Prof. Lies Bouwman is kindly acknowledged for the support and scientific discussion. Bart Jan van Kolck is kindly acknowledged for the supply of hydrogel slides for the giant vesicle experiments. NWO (The Netherlands Organization for Scientific Research) is acknowledged for a VIDI grant to S.B. The European Research Council is acknowledged for an ERC starting grant to S.B.

- [1] Q. Liu, W. Feng, T. Yang, T. Yi, F. Li, *Nat. Protoc.* **2013**, *8*, 2033.
- [2] a) J.-H. Kim, J.-H. Kim, *J. Am. Chem. Soc.* **2012**, *134*, 17478; b) P. Mahato, A. Monguzzi, N. Yanai, T. Yamada, N. Kimizuka, *Nat. Mater.* **2015**, *14*, 924.
- [3] a) J. Zhou, Q. Liu, W. Feng, Y. Sun, F. Li, *Chem. Rev.* **2014**, *115*, 395; b) T. N. Singh-Rachford, F. N. Castellano, *Coord. Chem. Rev.* **2010**, *254*, 2560.
- [4] a) S. Hisamitsu, N. Yanai, N. Kimizuka, *Angew. Chem., Int. Ed.* **2015**, *54*, 11550; b) S. H. Lee, D. C. Thévenaz, C. Weder, Y. C. Simon, *J. Polym. Sci., Part A: Polym. Chem.* **2015**, *53*, 1629; c) P. Duan, N. Yanai, H. Nagatomi, N. Kimizuka, *J. Am. Chem. Soc.* **2015**, *137*, 1887; d) P. Duan, N. Yanai, N. Kimizuka, *J. Am. Chem. Soc.* **2013**, *135*, 19056; e) A. J. Svagan, D. Busko, Y. Avlasevich, G. Glasser, S. Balushev, K. Landfester, *ACS Nano* **2014**, *8*, 8198.
- [5] a) J.-H. Kim, J.-H. Kim, *ACS Photonics* **2015**, *2*, 633; b) Z. Huang, X. Li, M. Mahboub, K. Hanson, V. Nichols, H. Le, M. L. Tang, C. J. Bardeen, *Nano Lett.* **2015**, *15*, 5552.
- [6] a) M. Majek, U. Faltermeier, B. Dick, R. Pérez-Ruiz, A. Jacobi von Wangelin, *Chem. - Eur. J.* **2015**, *21*, 15496; b) O. S. Kwon, J. H. Kim, J. K. Cho, J. H. Kim, *ACS Appl. Mater. Interfaces* **2015**, *7*, 318.
- [7] a) A. Monguzzi, S. M. Borisov, J. Pedrini, I. Klimant, M. Salvalaggio, P. Biagini, F. Melchiorre, C. Lelii, F. Meinardi, *Adv. Funct. Mater.* **2015**, *25*, 5617; b) A. Nattestad, C. Simpson, T. Clarke, R. W. MacQueen, Y. Y. Cheng, A. Trevitt, A. J. Mozer, P. Wagner, T. W. Schmidt, *Phys. Chem. Chem. Phys.* **2015**, *17*, 24826; c) S. P. Hill, T. Banerjee, T. Dilbeck, K. Hanson, *J. Phys. Chem. Lett.* **2015**, *6*, 4510; d) A. Nattestad, Y. Y. Cheng, R. W. MacQueen, T. F. Schulze, F. W. Thompson, A. J. Mozer, B. Fückel, T. Khoury, M. J. Crossley, K. Lips, G. G. Wallace, T. W. Schmidt, *J. Phys. Chem. Lett.* **2013**, *4*, 2073.
- [8] a) S. H. C. Askes, M. Kloz, G. Bruylants, J. T. Kennis, S. Bonnet, *Phys. Chem. Chem. Phys.* **2015**, *17*, 27380; b) S. H. C. Askes, A. Bahreman, S. Bonnet, *Angew. Chem., Int. Ed.* **2014**, *53*, 1029.
- [9] Q. Liu, T. Yang, W. Feng, F. Li, *J. Am. Chem. Soc.* **2012**, *134*, 5390.
- [10] A. Nagai, J. B. Miller, P. Kos, S. Elkassih, H. Xiong, D. J. Siegwart, *ACS Biomater. Sci. Eng.* **2015**, *1*, 1206.
- [11] a) C. Wohnhaas, V. Mailänder, M. Dröge, M. A. Filatov, D. Busko, Y. Avlasevich, S. Balushev, T. Miteva, K. Landfester, A. Turshatov, *Macromol. Biosci.* **2013**, *13*, 1422; b) C. Wohnhaas, A. Turshatov, V. Mailänder, S. Lorenz, S. Balushev, T. Miteva, K. Landfester, *Macromol. Biosci.* **2011**, *11*, 772.
- [12] a) Q. Liu, B. Yin, T. Yang, Y. Yang, Z. Shen, P. Yao, F. Li, *J. Am. Chem. Soc.* **2013**, *135*, 5029; b) O. S. Kwon, H. S. Song, J. Conde, H.-I. Kim, N. Artzi, J.-H. Kim, *ACS Nano* **2016**, *10*, 1512.
- [13] a) C. LoPresti, H. Lomas, M. Massignani, T. Smart, G. Battaglia, *J. Mater. Chem.* **2009**, *19*, 3576; b) D. E. Discher, A. Eisenberg, *Science* **2002**, *297*, 967; c) J. P. Jain, W. Y. Ayen, N. Kumar, *Curr. Pharm. Des.* **2011**, *17*, 65; d) D. E. Discher, F. Ahmed, *Annu. Rev. Biomed. Eng.* **2006**, *8*, 323; e) R. J. R. W. Peters, M. Marguet, S. Marais, M. W. Fraaije, J. C. M. van Hest, S. Lecommandoux, *Angew. Chem., Int. Ed.* **2014**, *53*, 146; f) S. Cavalli, F. Albericio, A. Kros, *Chem. Soc. Rev.* **2010**, *39*, 241; g) J. V. Georgieva, R. P. Brinkhuis, K. Stojanov, C. A. G. M. Weijers, H. Zuilhof,

- F. P. J. T. Rutjes, D. Hoekstra, J. C. M. van Hest, I. S. Zuhorn, *Angew. Chem., Int. Ed.* **2012**, *51*, 8339.
- [14] a) W. H. Binder, R. Sachsenhofer, *Macromol. Rapid Commun.* **2008**, *29*, 1097; b) M. Noor, T. Dworeck, A. Schenk, P. Shinde, M. Fioroni, U. Schwaneberg, *J. Biotechnol.* **2012**, *157*, 31.
- [15] J. E. Puskas, Y. Chen, Y. Dahman, D. Padavan, *J. Polym. Sci., Part A: Polym. Chem.* **2004**, *42*, 3091.
- [16] U. Karl, C. Sierakowski, M. Darijo, M. Haberer, H. Hartl, *US20080293886*, BASF Aktiengesellschaft, Ludwigshafen, Germany **2008**.
- [17] a) M. C. Woodle, M. S. Newman, J. A. Cohen, *J. Drug Targeting* **1994**, *2*, 397; b) M. C. Woodle, L. R. Collins, E. Sponsler, N. Kossovsky, D. Papahadjopoulos, F. J. Martin, *Biophys. J.* **1992**, *61*, 902.
- [18] B. X. Mi, Z. Q. Gao, C. S. Lee, S. T. Lee, H. L. Kwong, N. B. Wong, *Appl. Phys. Lett.* **1999**, *75*, 4055.
- [19] M. Almgren, *J. Am. Chem. Soc.* **1980**, *102*, 7882.
- [20] B. Kalman, N. Clarke, L. B. A. Johansson, *J. Phys. Chem.* **1989**, *93*, 4608.
- [21] a) S. H. C. Askes, N. L. Mora, R. Harkes, R. I. Koning, B. Koster, T. Schmidt, A. Kros, S. Bonnet, *Chem. Commun.* **2015**, *51*, 9137; b) M. Penconi, P. L. Gentili, G. Massaro, F. Elisei, F. Ortica, *Photochem. Photobiol. Sci.* **2014**, *13*, 48.
- [22] D. Bainbridge, M. Ediger, *Rheol. Acta* **1997**, *36*, 209.
- [23] A. Monguzzi, R. Tubino, F. Meinardi, *Phys. Rev. B* **2008**, *77*, 155122.
- [24] a) F. A. Carey, R. J. Sundberg, *Advanced Organic Chemistry*, 5th ed., Springer, US **2007**; b) B. Rånby, J. F. Rabek, *Singlet Oxygen Reactions with Organic Compounds and Polymers*, John Wiley & Sons, Ltd., NY, USA **1978**.
- [25] J.-H. Kim, F. Deng, F. N. Castellano, J.-H. Kim, *ACS Photonics* **2014**, *1*, 382.
- [26] a. A Meister, M. E. Anderson, *Annu. Rev. Biochem.* **1983**, *52*, 711.
- [27] G. R. Buettner, *Arch. Biochem. Biophys.* **1993**, *300*, 535.
- [28] F. Wilkinson, J. Schroeder, *J. Chem. Soc., Faraday Trans. 2* **1979**, *75*, 441.
- [29] M. Y. Li, C. S. Cline, E. B. Koker, H. H. Carmichael, C. F. Chignell, P. Bilski, *Photochem. Photobiol.* **2001**, *74*, 760.
- [30] M. Roche, P. Rondeau, N. R. Singh, E. Tarnus, E. Bourdon, *FEBS Lett.* **2008**, *582*, 1783.
- [31] a) H. J. Feldmann, M. Molls, P. Vaupel, *Strahlenther. Onkol.*, **1999**, *175*, 1; b) P. Vaupel, F. Kallinowski, P. Okunieff, *Cancer Res.* **1989**, *49*, 6449; c) E. E. Graves, M. Vilalta, I. K. Cecic, J. T. Erler, P. T. Tran, D. Felsner, L. Sayles, A. Sweet-Cordero, Q.-T. Le, A. J. Giaccia, *Clin. Cancer Res.* **2010**, *16*, 4843.
- [32] a) S. Zhang, H. Gao, G. Bao, *ACS Nano* **2015**, *9*, 8655; b) G. Sahay, D. Y. Alakhova, A. V. Kabanov, *J. Controlled Release* **2010**, *145*, 182; c) N. Oh, J.-H. Park, *Int. J. Nanomed.* **2014**, *9*, 51.
- [33] J. Schindelin, I. Arganda-Carreras, E. Frise, V. Kaynig, M. Longair, T. Pietzsch, S. Preibisch, C. Rueden, S. Saalfeld, B. Schmid, J.-Y. Tinevez, D. J. White, V. Hartenstein, K. Eliceiri, P. Tomancak, A. Cardona, *Nat. Methods* **2012**, *9*, 676.
- [34] a) L. B. A. Johansson, Y. G. Molotkovskii, L. D. Bergel'son, *J. Am. Chem. Soc.* **1987**, *109*, 7374; b) R. O. Al-Kaysi, T. Sang Ahn, A. M. Muller, C. J. Bardeen, *Phys. Chem. Chem. Phys.* **2006**, *8*, 3453.
- [35] A. Minsky, A. Y. Meyer, M. Rabinovitz, *J. Am. Chem. Soc.* **1982**, *104*, 2475.
- [36] N. Lopez Mora, J. S. Hansen, Y. Gao, A. A. Ronald, R. Kieltyka, N. Malmstadt, A. Kros, *Chem. Commun.* **2014**, *50*, 1953.

Received: May 20, 2016  
Revised: July 12, 2016  
Published online: August 29, 2016